https://doi.org/10.1595/205651324X16826780236175 *Johnson Matthey Technol. Rev.*, 2024, **68**, (1), 71–90

JOHNSON MATTHEY
TECHNOLOGY REVIEW

technology.matthey.com

Porous Metallic Implants from Additive Manufacturing to Biocorrosion: A Review

Trends and perspectives in additively manufactured synthetic orthopaedic implants

Salwa El Baakili, Patrick Munyensanga, Meriame Bricha, Khalil El Mabrouk*
Euromed Research Centre, Euromed Polytechnic School, Euromed University of Fez, BP 51, Main Fez, Morocco

***Email:** k.elmabrouk@ueuromed.org

PEER REVIEWED

Received 9th December 2022; Revised 22nd March 2023; Accepted 28th April 2023; Online 28th April 2023

The improved bulk and surface function of manufactured implants has advanced implantation procedures, leading to a decline in surgical risks. Many current techniques discussed in the literature are related to additive manufacturing (AM) of lightweight implants based on reliable, precise, flexible scaffolds and capable of mimicking bone properties while incorporating other useful features. These techniques have evolved for the production of a variety of biocompatible materials. AM has progressed beyond prototype to full-scale manufacturing of metals, polymers and ceramic products. However, metallic implants often fail *in vivo* due to biocorrosion and deterioration, limiting implant longevity. This study reviews current trends and approaches to enhancing the surface corrosion resistance of porous metallic implants and the effect of interfacial films on biological activity. The art of porous metallic implants manufactured by AM and their biocorrosion behaviour are discussed. This review also evaluates future trends and perspectives in additively manufactured synthetic orthopaedic implants porous with enhanced surface morphology.

1. Introduction

For centuries, Hindu surgeons repaired defective organs on the body's surface. Anaesthesia and asepsis were performed to limit excessive damage to these living organs (1). This operation has been practical since 600 BCE, when Susrutha, a surgeon, replaced an injured nose with flesh from the cheek region. This orthopaedic practice was used for replacing living flesh from a healthy organ to a wounded one (1, 2). From 1565 until the 1860s, the application of metals in aseptic surgical procedures was limited to certain structures. Wires and pins made of iron, gold, platinum, silver and other metals were used as raw materials. However, these materials present imperfections after implantation and often fail in tissue transplantation. In the 19th century and during World War I, many techniques were elaborated to heal wounds, including closure and tissue transfer surgery. The researchers Von Graefe and Gillies in the UK, Davis, Ivy and Kazanjian in the USA and Filator became the first to study these techniques (3). From 1893 until the 1920s, UK researcher Lane designed a fracture plate from type 316L stainless steel with improved effectiveness in the physiological environment and higher corrosion resistance in contact with body fluids than previous alloys. In the following years, other metal alloys were developed with excellent biocompatibility and mechanical properties, such as cobalt-chromium in the 1930s, pure titanium

© 2024 Johnson Matthey

and nickel-titanium alloys. These materials were widely used for implant fabrication over the following decades. **Table I** provides brief details of the historical development of biomaterials (1, 4).

Nowadays, AM offers many advantages, including high degrees of geometric freedom and short production periods. Compared to traditional methods, AM can produce parts more quickly, which can be particularly helpful in emergency medical situations. For example, bioprinting techniques can reduce time consumption during machining and material handling. When it comes to the biocorrosion of metals, AM has many advantages over traditional manufacturing processes like casting, extrusion, grinding and mechanical abrasion (5), such as design flexibility. It allows complex shapes and geometries to be produced with various materials and architectures that would be challenging or impossible to create with conventional techniques. This is particularly helpful in biomedical settings requiring individual patient-specific implants or prosthetics (6). Moreover, AM enables precise control over the quantity of materials used during production, which can aid in reducing waste and making the process more environmentally friendly. In addition, AM produces parts with a smoother surface finish, which can be crucial for lowering the risk of corrosion and infection in biomedical applications (7, 8).

According to the International Organization for Standardization (ISO), AM is a "process of joining materials to make parts from 3D model data, usually layer upon layer, as opposed to subtractive manufacturing and formative manufacturing methodologies" (9).

AM techniques have evolved to fabricate diverse material types including metals, polymers and ceramics (10). Two major advantages for manufacturing medical devices with complex shapes can be summarised as 'batch-size-indifference' and 'complexity-for-free' (11). Zadpoor defined batch-size-indifference as producing biomedical products for orthopaedic and plastic surgery applications that mimic the natural disorder in living organs (10, 11). At the same time, complexity-for-free enables the creation of multiple device designs with complicated geometries, enhanced features and advanced functionality. Porous implants are based on a lattice structure as the repeated unit cells according to 3D directions (10), presenting a notable improvement in mechanical and biological properties, such as mass transport, permeability, diffusivity and tissue regeneration rate after implantation surgery.

The design of porous implants based on AM enables topology optimisation to produce a lightweight implant with maximised stiffness, improved fatigue strength and increased longevity after implantation (12). Metals, such as titanium (Ti-6Al-4V, Grade 23), can be used to fabricate dense and porous implants. These materials possess good mechanical properties, corrosion

Table I Major Historical Developments of Biomaterials (1, 4)

Year, Author	Activity
600 BCE, late 18th–19th century, Sushruta Samhita	Nose reconstruction; various metal devices to fix fractures: wires and pins made of iron, silver and platinum
1860–1870, Lister	Aseptic surgical techniques developed
1893–1912, Lane	Steel screws and plates for fracture fixation
1912, Sherman	Vanadium steel plate, a first alloy developed exclusively for medical use; less stress concentration and corrosion
1926, Hey-Groves	Used carpenter's screw for femoral neck fracture fixation
1926, Large	18/8s Mo stainless steel (2–4% molybdenum) for greater corrosion resistance than 18/8 stainless steel
1931, Smith-Petersen	Designed first femoral neck fracture fixation nail made originally from stainless steel, later changed to vitallium
1938, Wiles	First total hip replacement
1946, Judet and Judet	The first use of biomechanically designed hip prosthesis; first use of plastics in joint replacements
1958, Charnely	The first use of acrylic bone cement in total hip replacements
1958, Furman and Robinson	First successful direct stimulation of the heart
1960, Starr and Edwards	Heart valves
1980, Kolff *et al*.	Artificial heart

© 2024 Johnson Matthey

resistance and low specific weight. Their excellent strength-to-weight ratio compared to other metals with good biocompatibility makes them useful for medical implants (13, 14). Cobalt-chromium (UNS R31538/ASTM F1537-20) is used extensively in high-load areas due to its high stiffness (15, 16).

Stainless steel (316L) has been investigated in AM as a metal implant for surgical applications with excellent wear properties, good mechanical properties at temperatures above 500°C and good corrosion resistance, including pitting corrosion and exposure to chloride environments (17, 18). Recently, three-dimensional (3D)-printed tantalum has gained more attention for biomedical applications due to its biocompatibility and the presence of a self-passivating surface oxide layer, which is beneficial for biological applications (19). Different chemical structures formed *in situ* after the AM process explain the behaviour of such biomaterials during their application.

Apart from the various metallic implant materials used, their intrinsic qualities and the biointerface between implant and bone tissue, implant performance also depends on the quantity and quality of the host tissue. For instance, corrosion behaviour is a significant consideration in the design and selection of the material. A variety of corrosion mechanisms can cause implant loosening and failure. As a result, before being approved by regulatory organisations, biomaterials are required to be tested for corrosion and solubility. The study of corrosion behaviour of selective laser melted Ti-6Al-4V alloy in sodium chloride showed unfavourable corrosion resistance of the produced samples related to the large amount of acicular α-phase and lower amounts of β-phase. Titanium ions express high resistance to corrosion due to the spontaneous formation of a compact and chemically stable oxide film on the metal surface (passivation inhibitors) (20). Li *et al*. found that the corrosion fatigue behaviour of porous zinc based on diamond unit cell was higher than the uniform structure in different media (21).

The current study first reviews the AM of porous metallic implants manufactured by the powder bed fusion (PBF) process; after that, the biocorrosion behaviour of these implants in contact with body fluids is discussed.

2. An Overview of Powder Bed Fusion Process Applications

AM technology has gained significant attention due to its advantages over traditional subtractive fabrication technologies. AM allows the creation of exceptionally complex parts in a short lead time without additional tools or moulds (22). Therefore, it is appropriate for producing low-volume parts with high shape complexity, multiple functions and the ability to make monobloc parts (i.e., parts that do not require assembly) (23). However, this technology has significant limitations, such as lower productivity than traditional methods and the ability to make parts only at small and medium scales (10, 22).

Several AM processes have been used to fabricate patient-specific implants for bone replacement, including the binder spraying process (3D printing), fused deposition modelling and laser powder densification (selective laser sintering (SLS), selective laser melting (SLM)). The latter uses a laser beam to densify material powders such as polymer, ceramic, metal or a mixture locally and then uses an ultraviolet laser beam to polymerise a liquid photosensitive resin (stereolithographic) into a solid polymer (24, 25). Porous metallic implants are mainly fabricated through one of three manufacturing techniques, namely directed energy deposition (DED), binder jet (BJ) and PBF. The difference between the techniques is the heat source (26). DED is based on an ejection of metal powder from a moving nozzle which is then sintered by a mobile energy source such as a laser beam. In contrast, BJ requires a preliminary step to mix the metal powder with a specified binder. Then the 3D structure is created by depositing the mixture with a mobile nozzle. Finally, the part is sintered and the binder is removed. In the case of PBF, the part is built in a powder bed. Then the energy source (laser or electron beam) is used to selectively sinter the desired areas to form the final part (24, 27, 28). These techniques generally involve heating metal powders from several melt pools that consolidate through a rapid solidification process (29, 30). **Table II** summarises the relevant AM technologies used for porous metallic implants and their features (31).

In the biomedical industry, two primary powder-based fusion technologies for metal AM are most used: electron beam melting (EBM) and SLM. According to computer aided design (CAD) data implantation, both techniques use a high-temperature directed energy source (either an electron beam or a laser beam) to melt and bond a thin layer (20–200 μm) of fine metal powders. Each layer cools before bonding to the previous one (36). Then the selected regions of metal powder are bonded layer by layer until

© 2024 Johnson Matthey

Table II Additive Manufacturing Technologies (31)

Metallic additive manufacturing processes	Advantages	Disadvantages	References
Binder jetting	Ability to create shapes that are difficult or impossible for traditional methods; no need for potentially extensive laser optimisation experimentation; no heat source is used during the processing; no need for a build plate	Need post-processing; considerable porosity exists; not available for part reparation	(32)
Selective laser melting	Capable of fully melting the powder material, producing fully dense near-net-shape components without the need for post-processing; high processing precision (≤10 μm)	Support is needed; high quality demands for metal powders; limited part size; distortion caused by residual thermal stress; not available for part reparation	(33)
Electron beam melting	Kinetic energy transfer and preheating the powder result in lower thermal stresses; vacuum environment; metal does not oxidise easily; no support is needed	Complex internal cavities are not possible due to preheating/ sintering process; rougher texture and less precise than laser beam manufacturing	(34, 35)
Direct energy deposition	Part size is not limited to bed size; large metal parts; good material utilisation; multiple wire feed nozzles can be used with a single electron beam gun	Lower processing accuracy than powder bed AM; poor surface finish	(26, 34)

the required metal implant is entirely built. The implants are manufactured in sterile environments and the metal powders that are not melted can be recycled and reused. However, SLM and EBM technologies have demonstrated the potential to fabricate porous metal scaffolds with reduced fabrication time, excellent dimensional accuracy, a clean construction environment and near-net-shape capability (6).

2.1 Selective Laser Melting

The SLM technique consists of melting a thin layer of metal powder using a high-power laser. It involves several steps, from digital design data preparation to removing the completed part. First, CAD and computer aided manufacturing (CAM) software create the data for each layer. The CAD/CAM data is then transferred to the SLM machine and the printing operation begins with applying a thin layer of metal powder to a plate. At the same time, the piston is set to its highest position at the start of the printing process (6). Immediately after the powder is laid, a high-energy laser beam traces a two-dimensional section on the powder's surface, followed by instantaneous solidification after the laser is turned off. The plate that supports the current 3D model drops by the thickness of the layer created by the powder feed cartridges and adjusts its level to that of the plate. A new layer of powder is spread, and the process is repeated until the 3D model is obtained. Finally, the completed 3D part is manually removed from the platform or by electrical discharge machining and any remaining powders are removed from the surface (33, 37).

To mimic the structure of natural bone and encourage bone growth into the implant, porous implants can be made with controlled pore size and interconnectivity. Due to the implant's porosity, drugs or growth factors that promote bone regeneration may also be delivered. Additionally, biocompatible metals like titanium and its alloys can offer mechanical strength and corrosion resistance which are crucial for long-term implant stability and biocompatibility (38).

Today, SLM is the most prevalent metal powder bed melting technique for producing metal biomaterials (39). This is consistent with the growth of SLM in developing new machinery and innovation to make it more productive and economically attractive. For instance, it is possible to mimic bone architecture and approach its structure with SLM. Limmahakhun *et al*. studied the effect of microporous structure and mechanical properties of cobalt-chromium alloy scaffolds produced by SLM. They reported that SLM techniques could fabricate cobalt-chromium cellular structures with graded beam thickness

 © 2024 Johnson Matthey

similar to human bone's mechanical properties and morphology (40, 41).

Several studies have shown the fabrication of porous metallic implants by SLM with successful *in vitro* and *in vivo* outcomes (42). For instance, studies favour PBF techniques for manufacturing bone graft substitutes that balance mechanical function and biological performance. Wang *et al*. (43) produced implants tested *in vitro* and *in vivo* by applying different topology designs and fabrication methods. Chen *et al*. (44) manufactured an implant by SLM. They achieved better compressive strength than that of human cancellous bone, which is 100–250 GPa, and their stiffness values indicated less elasticity than that of human cortical bone with 1.5–11.2 GPa. Fully dense titanium alloy implants have a contact strength of 115 GPa of bone-to-implant (osteointegration) and bone volume fraction. There were improved results in a rabbit model for porous titanium implants made by SLM compared to solid implants. An adequately designed porous scaffold can accelerate the osseointegration process and the use of CAD and AM techniques can potentially improve the traditional porous scaffold approach and cell morphology attachment, viability and proliferation. In addition, the manufactured implants were suitable for the regeneration of bone ingrowth and integration (42). Another study showed that porous titanium implants fabricated by SLM with a gradient pore structure could enhance osteogenesis and angiogenesis in a rat model (43). The SLM process can be precisely controlled, allowing for the creation of highly complex geometries and intricate porous structures which target biomedical engineering applications.

2.2 Electron Beam Melting

EBM is one of the PBF processes, where the electron beam is obtained by heating under vacuum a tungsten filament. Then, electrons accelerated and directed by electromagnets are projected at high speed on the powder surface. The powder is thus brought to the melting point. As its name indicates, the difference with the previously mentioned process is using an electron beam instead of lasers (45).

In 2015, the Swedish company Arcam AB developed the EBM process method, a widely used powder bed melting technique for metals like SLM. The system comprises a rake, a construction platform, powder hoppers and a power source. However, the system uses the energy of an electron beam rather than a laser. Recently, EBM research has become more competitive with SLM. The use of EBM is considered desirable for biomedical parts due to the consistency of its energy beam. The high power of the electron beam improves the ability to manufacture products with lower residual stress but higher surface roughness, meaning that low residual stress is achievable in high-temperature processes. Economically, metal-AM procedures are inflexible concerning the handling of inputs, including the characteristics of the metallic powder to be used (46). It was reported that the load-bearing components for Ti-6Al-4V manufactured by the EBM process have excellent mechanical properties equal to that of the parts made by a forging process (47).

The ability to design highly porous structures with precise pore sizes, shapes and interconnectivity is one of the major benefits of EBM and SLM. In addition, improved osseointegration (the process by which bone tissue grows into the implant) and vascularisation (the process by which blood vessels grow into the implant) are made possible by the ability to customise the porosity to the particular needs of the implant. Infiltration of cells and tissue is also possible due to the interconnected porosity, which enhances the integration of the implant with the surrounding tissue (38).

Several findings show that EBM has the ability to create porous implants of superior quality and with superior mechanical and biological properties. These implants' high porosity and linked pore networks are perfect for encouraging osseointegration, which is essential for long-term stability, function and bone ingrowth (48). In research conducted by Crovace *et al*., porous titanium implants made by EBM were assessed using a sheep model. The implants had excellent biocompatibility and bone tissue integration. According to the authors, there were no indications of implant failure or unfavourable reactions (49). Szymczyk-Ziółkowska *et al*. (50) examine the impact of various processing parameters on the mechanical and microstructural characteristics of porous titanium implants produced by EBM. The authors discovered that varying the laser's strength and scanning rate could control the size and distribution of the implants' pores. Additionally, they explain that increasing implant porosity led to lower stiffness but higher toughness, which may be advantageous for some uses.

The general standard for metallic biomaterials to be handled effectively using the powder bed combination is that the material must be suitable for

© 2024 Johnson Matthey

casting and welding. Subsequently, economically accessible metal powders are often provided by AM. However, the SLM and EBM technologies can withstand a higher manufacturing rate than conventional processes (10, 51).

3. Corrosion Aspect of Three-Dimensional Printed Porous Implants

Over the years, corrosion has attracted researchers to study its behaviour in metals-related degradation, failure and significant accidents. Biocorrosion is relevant to medical applications. A variety of substantial complications occurs if the fabrication processes of bio-metal implants are not controlled. In an *in vivo* application, unwanted effects such as rashes and some carcinogenic symptoms are generated (52). An example is nickel ions alloyed in cobalt-chromium-molybdenum which, if released above the limit of the applied area, can cause heart problems and brain disorders (especially in pregnant women) (52). To overcome this biomaterial degradation *in vivo* application, AM suggests various post-processing methods to protect and improve the material by creating an interfacial layer by heat treatment, machining, abrasive blasting, sanding and painting. The most commonly employed process for the surface modification of implants found in the literature with noticeable results in the unique microstructure of the surface (53) is electrochemical deposition coating, which reduces the degradation of the passivated film and improves its corrosion resistance (54). The AM process might also accelerate common corrosion issues due to pores, molten pool boundaries, surface roughness and anisotropy of produced porous implants, especially in SLM (20, 55) and EBM (55). It has been expressed by Dai *et al*. that due to the presence of metastable α′-martensite (**Figure 1(a)**), the SLM sample of Ti-6Al-4V exhibited a more significant passive current density and a lower pitting potential in ~150 mV that is lower in chloride solution compared to the wrought equivalents (commercial Ti-6Al-4V) (20). The acicular α′-martensite was well dispersed throughout the microstructure, accompanied by some typical long and previously columnar β-grains (55, 56) (**Figure 1(b)**). The martensitic transition occurred due to the extremely high cooling rate as the SLM-manufactured Ti-6Al-4V exhibits higher passive current density and a lower pitting potential. Furthermore, the volume fractions of the β-phase for commercial and Ti-6Al-4V alloy samples by SLM were 13.3% and 5.0%, respectively (20). It is well known that the β-phase contains more vanadium and that the oxide layer generated becomes more stable than that formed on the α-phase, both contributing to corrosion resistance (57).

Passivation is considered a non-electrolytic self-process to improve metal and alloy corrosion and rust resistance (53). However, when electrolytic current induced after specimen manufacturing is combined with chemical decomposition of metallic ions such as iron, chromium and other nonferrous metals, passivation techniques might depend on the specific alloy (58). One example used sulfate adsorption to enhance reductivity in the dissolution of the monolayer film (passive) and layer with cations (H^+) and facilitate the process by

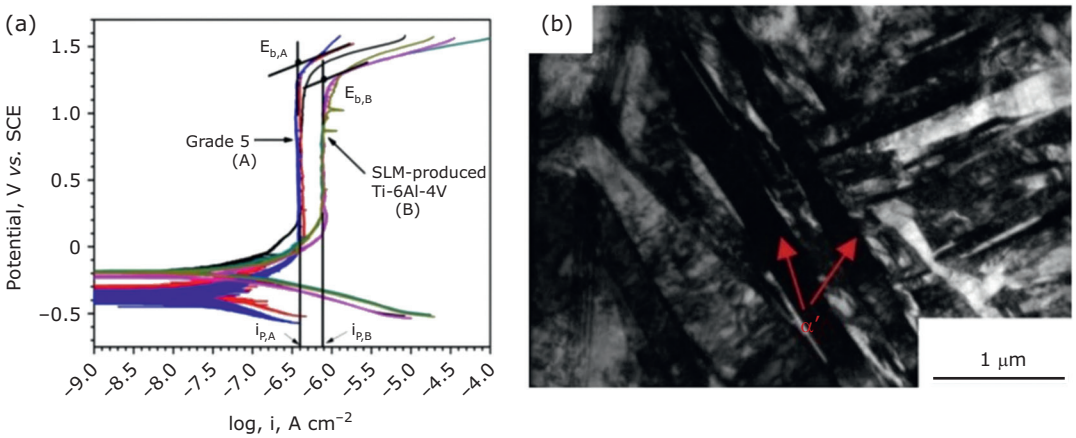

Fig. 1. (a) Potentiodynamic polarisation curves for the SLM Ti-6Al-4V alloy and commercial Grade 5 alloy in 3.5 wt% NaCl solution. Reprinted from (20), Copyright (2016), with permission from Elsevier; (b) bright-field transmission electron microscopy (TEM) image of the as-received SLM Ti-6Al-4V alloy. Reprinted from (55), Copyright (2016), with permission from Elsevier

 © 2024 Johnson Matthey

making it permeable (59). The passivation effect has been observed quantitatively based on the formation of ion discharge in the presence of oxide formed in a quasi-equilibrium process involving a singleton electron change (60). As a result of failed passivation of porous metal implants, several surface functionalisation techniques might be used to validate parameters involved in coating processes initiated for corrosion resistance. This has been explained by Dehghanghadikolaei *et al*., who used potentiodynamic polarisation to verify the coating process' behaviour applied on an implant's interfacial surface (61). Thus, it is advisable to use standard simulated body fluids (SBFs), which contain sodium chloride, a predominant of component of SBFs that react on the materials' surface resulting in corrosion during metal oxidation (58, 62). Surface corrosion can be reduced using nanocoating technology. The technique offers surface hardness from adhesive strength between both boundary layers of substrates with a nanoscale size of less than 100 nm and high density with good adhesion of the coated surface particles and high corrosive resistance with enhanced tribological properties. **Figure 2** shows these fine and compact/dense microstructures with few nanopores scattered through the surface treated with alkaline electrolyte under a voltage of 150 V.

Surfaces with uncontrolled large pores allow the penetration of corrosive media to the lower layers of the coating and make it more complex (61). Treatment of the parts' surface with different media, whether acidic or alkali, has been recommended for the investigation of corrosion and to enhance their resistance based on the mechanical properties of the porous implants. In some areas of the substrate, the microstructure of the coating layer is discontinuous, while in others, a fine microstructure might form, especially while polishing the surface. For example, in **Figure 2**, the surface inhibited the deposited ridge indicated by red arrows, whereas white arrows indicate their discontinuity, shown by a black hole on the surface.

Azzouz *et al*. electrophoretically coated Bioglass® 45S5 on Ti-6Al-4V, a prosthetic alloy, using controlled parameters such as an ideal voltage of 30 V and two deposition times of 30 s and 90 s. The coated surface was thermally heated for an hour at 120°C and 450°C, respectively, to provide a uniform coating, then crushed until a drop from 85 µm to 21 µm (63). Another technique is to treat the surface to both increase bioactivity with a bioabsorbable interfacial coating layer and improve corrosion resistance using an interfacial layer of the core metallic implant. Corrosion downgrades the implant's *in vivo* applications compared to the bulk properties and considerably affects the biocompatibility and regeneration of living bone (64). Thus, the corrosion resistance of AM implants is a broad concern. The appropriate AM process must be chosen to achieve specimens with an acceptable visual appearance, fewer surface porosities, high mechanical and physicochemical performance and good biocompatibility.

Further research conducted by Seyeux *et al*. illustrates various surface chemical analysis techniques recommended for surface modification

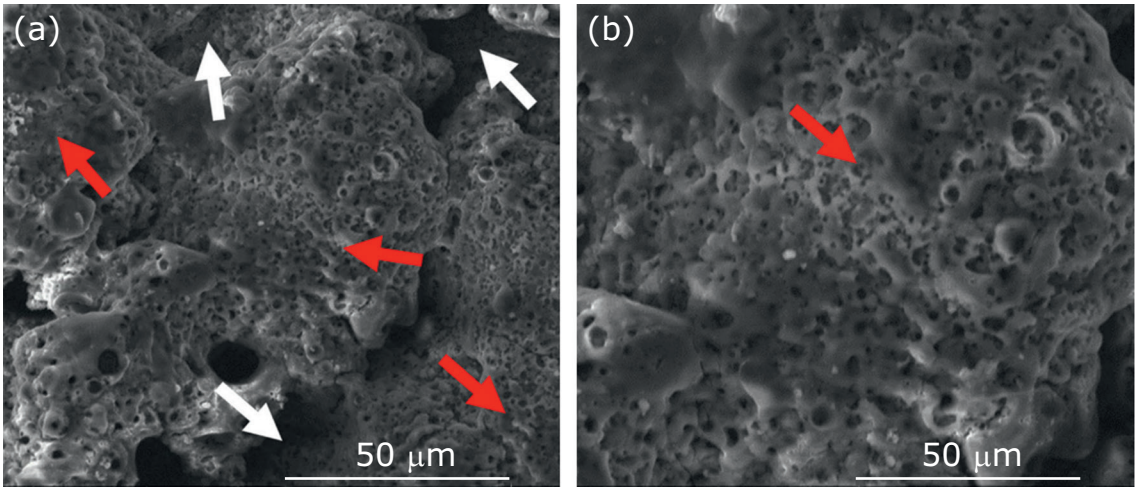

Fig. 2. Scanning electron microscopy (SEM) micrograph of the coating structure of an SLM printed sample coated in alkaline electrolyte under a voltage of 150 V at: (a) × 500; and (b) × 1000. Reprinted from (61) with permission from Springer Nature

© 2024 Johnson Matthey

and functionalisation. It is necessary to analyse surface chemistry to identify species formed that interact with the environment due to enhanced reactivity of the surface-forming chemical species. These techniques help to investigate any change in the chemical interfacial film of implants during biofilm growth (host integration). Using these techniques, the surface of porous implants in the biological medium can be analysed, the species present on the surface identified and evaluated, the oxidation state, depth of the profile and surface molecular species formed during the implant's integration identified (65). The mechanical behaviour of the surface, however, must be fully characterised. The surface analysis performed on Ti-6Al-4V hip implants explains the cyclic stress and corrosion causing 90% of surface fracture and the mechanical failure of dense and metallic porous implants (tribocorrosion). Cyclic loading accelerates corrosion due to the removal of passive films. The corrosion process can be explained as an electromechanical reaction driven by thermodynamic forces in body fluids near the implant's surface (66). The ionic strengths of cobalt, chromium and titanium ions, considered to be passive materials, are such that they form suitable barriers against metal oxides with a thickness of about 1 nm to 10 nm degradation of oxide films (67, 68). Prasad *et al*. provides a detailed analysis of these electrochemical reactions due to thermodynamic causes (69).

3.1 Concept of the Corrosion of Implant Materials

Electrochemical dissolution and wear-accelerated corrosion, or a combination of both, cause species degradation and impact the entire passive film of implants. Localised erosion affects specific regions, shielding the implant from physiological fluids and resulting in a crevice or pitting corrosion (1). These effects randomly affect a part of the films and create minor dents (microcracks) from a localised electrochemical or mechanical failure (70) due to the deterioration of the passivated oxide film (71). Extensive testing should be done in 3.5 wt% sodium chloride at room temperature (20) with electrochemical corrosion measurement due to unstable chemical oxide film formed on the metal surface. Dai *et al*. conducted a test three times for data reproducibility on various parameters to meet the required parameters, identifying the corrosion resistance of SLM-produced Ti-6Al-4V alloy in sodium chloride (20). The open circuit potential (OCP) was recorded during the stabilisation of the alloy sample, and the potentiodynamic polarisation test sweep range was set between −0.5 V and 1.6 V *versus* the OCP of 0.1667 mV s^{-1}. The electrochemical impedance spectroscopy was found at OCP potentiostatically when the electrochemical impedance spectroscopy was running by alternating current (AC) amplitude of 10 mV over the frequency range about 10^{-2} Hz to 10^{5} Hz (**Figure 1(a)**). In addition, mild corrosion that is selectively found to lead to the replacement of implants before the healing process is associated with toxic symptoms in the host (1).

Corrosion can be seen as an enemy of the beauty of metal parts produced in manufacturing; more on this was in the famous book of Fontana and Greene in 1967, after McKay and Worthington, who have studied numerous ways to prevent corrosion. Several authors have discussed various forms of corrosion and identified multiple types by visual observation on the surface films of implants or affected specimens (72). All forms are interrelated or unique based on symptoms ranging from a localised regions to a corroded area (1). Forms of corrosion in metallic implants were reviewed in detail regarding their chemical characteristics, mechanisms (thermodynamic force, kinetic barriers) and preventive measures in the host appliance (1, 72–74). The first and most prevalent type of corrosion is uniform attack, characterised by a uniform electrolytic discharge of species throughout the entire surface. The metal implants degrade under the exposed surface. The surface can be protected by overusing passivation (enhance inhibition reactions) or electrolytic reactions to prevent corrosion. The other form of corrosion, the galvanic type, affects two metals immersed in a solution under conductivity and produces a potential electron flow connection within the two metals. Both metals change phase from less corrosion-resistant to cathodic, while phases that are more resistant to corrosion should possess anodic species (75). Bowden *et al*. proved this theory in an experimental study by drilling stainless steel plates with a screwdriver. Significant ions from the screwdriver heads were transferred to drill-bit and drill-bit to stainless steel plates under electrochemical reaction (72).

Another example is cobalt-chromium alloys, widely used in implant manufacturing as total joint replacements. This alloy has a degradation ability to release ions of Co^{2+}, Cr^{3+} and Cr^{6+}, even though it has superior mechanical properties and wear resistance *in vivo*. Numerous studies try to

 © 2024 Johnson Matthey

solve these problems through the electrochemical deposition of species such as tantalum, materials reinforced by hydroxyapatite (HA) or by covering corroding films with mesoporous bioactive bioglass (68, 76). Singh *et al*. improved biocorrosion of the interfacial surface of cobalt-chromium alloy coated with tantalum-reinforced HA to increase surface hardness and were able to shift the potential of corrosion (E_{corr}) and reduce corrosion intensity (I_{corr}) (77). Their study shows that coating cobalt-chromium alloy with tantalum produces lower corrosion resistance than tantalum-reinforced HA, which reduces I_{corr} to 7.24 at 26% of HA-10Ta, HA-20Ta and HA-30Ta (78). The tantalum-coated specimens showed microcracks during characterisation with Ringer's solution (65), while the tantalum-reinforced HA coatings effectively offered the true morphological integrity of biocorrosion resistance. The study proposes a deeper investigation of the biological effect on bioresorbtion of released ions *in vivo* (78). Other types of corrosion, such as crevice corrosion, pitting corrosion, intergranular corrosion, selective leaching, erosion or fretting corrosion and stress-corrosion cracking, have been reviewed in depth for their causes and deterioration of metallic materials by Balamurugan *et al*. and Brown *et al*. (1, 79).

3.2 Corrosion Viability Throughout the Manufacturing Process

AM technologies have highlighted the potential of SLM and EBM. These methods allow the fabrication of porous implants and complex structures with adjustable elastic modulus with interconnected pores and implants with complicated interior and exterior shapes that are simple, fast and accurate at microscale (10). Conversely, conventional manufacturing techniques cannot control the geometrical parameters related to the pore structure and provide lower mechanical properties (80). For instance, in 2019, Yu Guo *et al*. studied the effect of novel selective laser-melted porous titanium-tantalum-niobium-zirconium alloy scaffolds on bone regeneration. This investigation compared scaffolds manufactured using traditional methods and printed by SLM. The conventional methods presented many disadvantages such as irregular pore size, unsuitable mechanical features and poor connectivity, unlike porous titanium-tantalum-niobium-zirconium scaffolds, which show a controllable pore size of 300–400 μm and enhanced mechanical properties, as well as osteogenesis and osteointegration (81–83). Similarly, B. Zhao *et al*. studied the corrosion resistance of Ti-6Al-4V alloy scaffolds fabricated by EBM and SLM for *in vivo* implantation. The result suggested that the corrosion resistance of the SLM specimen was best under low electric potential (≤1.5 V). In contrast, the EBM specimen was prominent under a high electric potential of ≥1.5 V. However, based on the result of the immersion tests, the corrosion resistance of the SLM specimen was better than that of EBM. The EBM specimen was affected by the content of titanium, aluminium and vanadium ions, while the SLM wrought specimens were shallow. The scaffolds produced by EBM and SLM had good corrosion resistance. Their corrosion rates are low and much less than the American Association of Corrosion Engineers (<0.05 mm $year^{-1}$) (84). In addition, electrochemical studies made by Zadeh *et al*. revealed that the better corrosion performance of the PBF manufactured alloy was mainly due to the formation of local galvanic cells in the EBM-manufactured Ti-6Al-4V alloy. Corrosion current densities of the PBF and EBM manufactured alloys after 100 h of immersion were 0.36 μA cm^{-2} and 0.87 μA cm^{-2}, respectively (85).

The quality of AM parts depends on manufacturing process parameters such as laser power (electron beam), scanning speed, powder size, powder layer thickness, scanning route and hatch space (86) (**Figure 3**). In particular, laser power variation impacts the corrosion resistance in a corrosive environment (3.5% NaCl). For example, a high laser power (190 W) significantly decreased the corrosion rate. Alternatively, stress-relief annealing led to a stabilisation of the corrosion potential E_{corr} (90). Marattukalam *et al*. achieved similar results when they studied the impact of laser engineered net shaping (LENS) processing parameters on nickel-titanium alloy's microstructure and corrosion characteristics for bone implants (91).

During the AM process, unique microstructures with refined grain structures, dislocation cells and internal residual stresses occur due to rapid heating and cooling rates combined with thermal cycling (formation of non-equilibrium phases with an extensive range of compositions). These conditions are not correctly controlled during the manufacturing process. As a result, they lead to metallurgical defects such as inclusion defects (**Figure 4**). During the solidification process, non-metallic particles called inclusions may become enmeshed in the metal framework (93). Impurities in the raw materials, insufficient cleaning of the environment or tools or poor process management can all contribute to these. Grain boundary defects

© 2024 Johnson Matthey

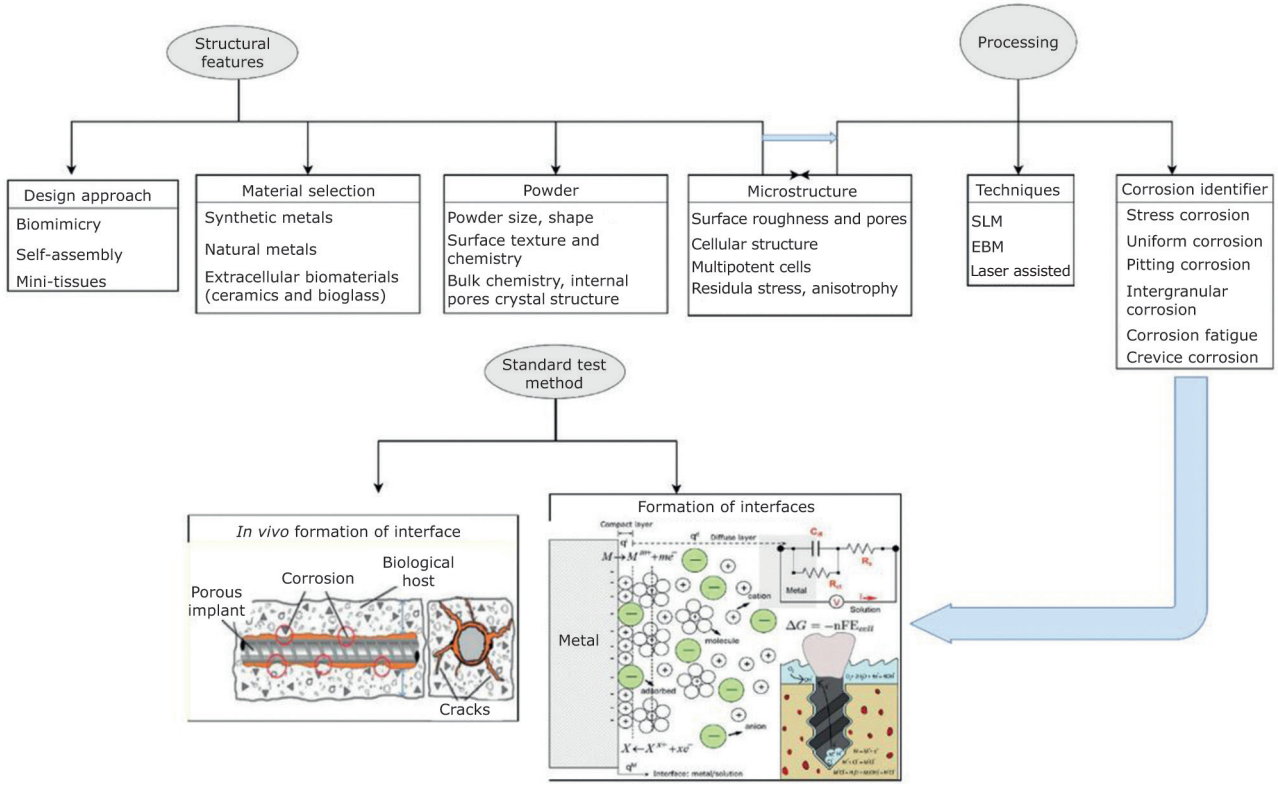

Fig. 3. Schematic diagram involving the powder, microstructure and related corrosion behaviour for AM-produced components and the standard test method for post-processing, electrochemical impedance measurement (EIM) to identify preoccuring corrosion based on host environments (53, 87–89)

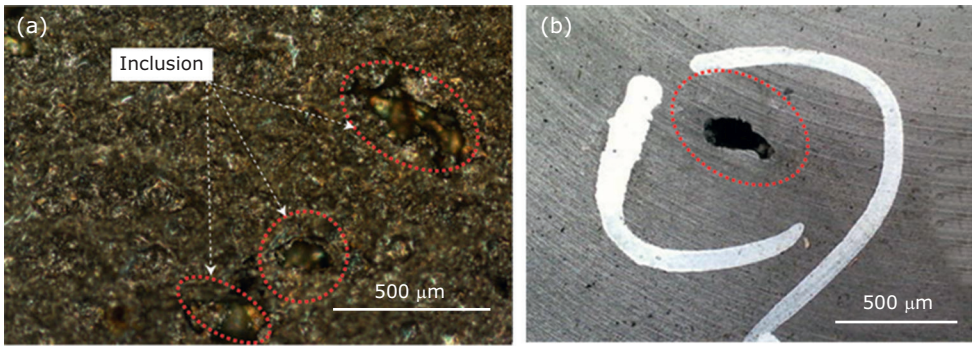

Fig. 4. Inclusion defect due to imperfect manufacturing process: (a) slag inclusion from SLM 316ST printed parts; (b) sand inclusion in casting due to sand crush or drop of mechanical force on the sand moulds or sand cores. Reprinted with permission from (92)

can also occur due to impurities or inclusions at the grain boundaries or uneven grain growth during solidification (53).

These flaws can weaken the substance, making it more prone to corrosion or failure. The existence of voids or gas bubbles within the metal matrix is referred to as porosity (38). This can be caused by insufficient melt degassing, inadequate shielding during welding or incorrect process settings. In addition, thermal growth or contraction during solidification or heat treatment can cause residual stresses. If not correctly managed, these stresses can cause deformation, cracking or other types of failure (94). These sites are preferential areas for corrosion. For example, surface roughness may happen when the melt flow is destabilised by gas expansion, resulting in a highly random and unstable melt pool with increased surface

 © 2024 Johnson Matthey

roughness and porosity. During laser melting, metallic droplets can develop in opposition to a desired uniform distribution of liquid metal over the melted surface (95, 96).

The crystallographic texture of a metal implant can also influence its corrosion behaviour because different crystal orientations can have varying susceptibilities to corrosion (97). Implants with specific crystal orientations may be more corrosion-resistant compared to others, which is critical for implant design and manufacturing. Thus, it is essential to understand the microstructure of materials produced by AM to predict their properties and to design implants with improved corrosion resistance. For example, some crystal orientations may have lower corrosion resistance due to grain boundaries or other defects that can act as sites for corrosion initiation. In addition, studies have shown that the crystallographic texture of AM-produced metal implants can be influenced by various factors, such as the direction of the laser beam, the scanning strategy and the powder characteristics. These factors can affect the crystal growth direction and the distribution of crystal orientations in the implant.

Another study investigated the effect of crystal orientation on the corrosion behaviour of 316L stainless steel produced by AM (93). A different study found that the crystal orientation of the material affected its corrosion behaviour, with materials that had a <100> crystal orientation showing better corrosion resistance than those with a <110> or <111> crystal orientation (98). This effect is due to the anisotropic nature of metal crystals, which means that properties such as corrosion resistance can vary depending on their orientation. For instance, some crystal planes may be more susceptible to corrosion than others due to their atomic arrangement (53).

3.3 Surface Condition and Microbiologically Influenced Biocorrosion

Surface conditions significantly impact the corrosion characteristics of materials interacting with the host environment. Localised corrosion attacks preferentially occur at irregular and rough sites on AM parts caused by large amounts of cavities (pores) and other surface defects (95). Microbiologically influenced biocorrosion generates a biofilm due to anodic and cathodic reactions from oxidation and reduction, respectively. Synergetic metabolic relationships between the host and interfacial surface of implants allow microorganisms from the biofilm to cause biodeterioration depending on the porous implant's physical and chemical conditions within the host (**Figure 5**). According to the findings of Leon and Aghion on the SLM AlSi10Mg alloy, the corrosion resistance of polished SLM components was considerably enhanced compared to the as-received AlSi10Mg alloy (99) due to optimisation of the physical stability of the surface.

Figure 6 explains a particular reaction due to metallic alloying in the bulk or porous implant microstructure. A different reaction occurs arbitrarily on the interfacial layer and the intermetallic phases or grain boundaries (**Figure 6(a)**). First, the $M(OH)_n$ (**Figure 6(b)**) layer covers the metallic alloy surface to absorb organic molecules (biofilm such as proteins, amino acids and lipids) and influence the biocorrosion process. Then, chloride adsorption breaks down the metallic layer and causes a new form of corrosion (pitting corrosion, **Figure 6(c)**) while calcium phosphate deposits onto the undissolved interfacial core layer and allows cells to adhere to the surface. These cells will progress the implantation and proliferate to form tissue adjacent to the corrosion (**Figure 6(d)**).

Comprehensive studies have explained the microstructure, macrostructure and evolution of defects during printing, thus, their impact on corrosion behaviour during implantation. Typically, pores are the first phenomenon that appears during the printing process, affecting the component's corrosion behaviour and surface roughness. Pores produced by SLM can be divided into two types: the first exist around unmelted powders, the second are formed by gas inside the powders during gas atomisation (101). The existence of pores compromises and accelerates the corrosion of the substrate (102). For example, Schaller *et al*. used a microelectrochemical test and found that pore sizes larger than 50 µm resulted in lower SLM 17-4 PH stainless steel pitting corrosion resistance. In contrast, pore sizes lower than 10 µm resulted in a passive state (103).

Additionally, pore geometry also has a significant impact on corrosion behaviour. Irregularly formed pores allow corrosion due to aggressive ion concentrations in the corners (103). The porosity of metallic scaffolds provides undeniable advantages since it ensures light weight and enhances biological properties (osteointegration and osteoconduction), cell adhesion and proliferation (104). Ran *et al*. conclude that tiny pores are helpful for cell adhesion. In contrast, large pores improve cell

© 2024 Johnson Matthey

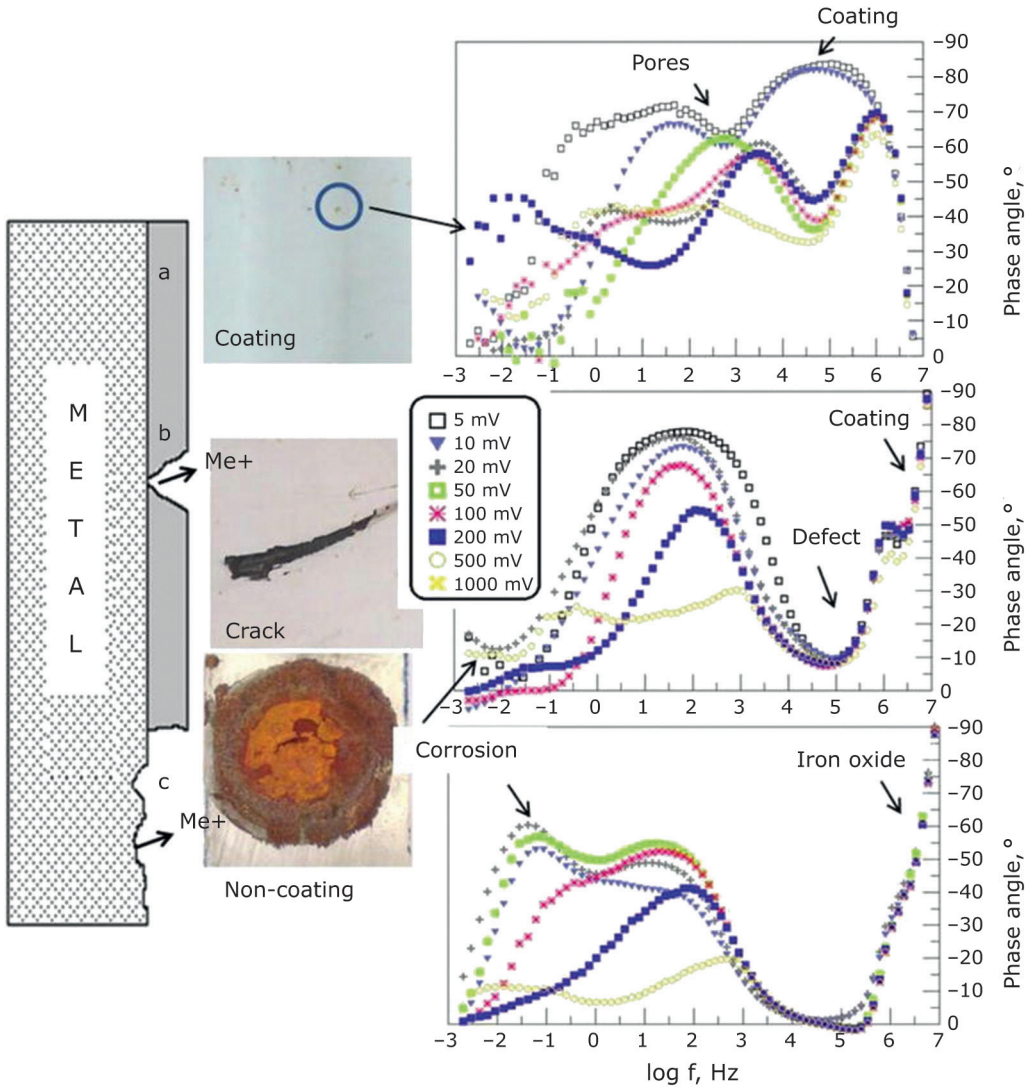

Fig. 5. Phase angle EIS response obtained for metal beverage containers at different surface conditions after immersion in 0.5 M NaCl as a function of AC amplitude signal: (a) uniform coating; (b) scratch defect on coating; (c) polished surface no-coating. Reprinted from (89) under Creative Commons Attribution 3.0 License (CC BY 3.0 DEED)

proliferation and pores of 600 μm are beneficial for bone ingrowth, maturation and bone-implant fixation stability (105). Likewise, pure porous tantalum implants additively manufactured by SLM show good functional implant-bone interface connection and high mechanical properties close to those of human bone and allow for bone ingrowth when evaluated after 12 weeks (106). However, a well-defined pore distribution with proper interconnectivity is needed not to counter the mechanical properties of fatigue resistance, high fracture toughness and corrosion resistance of the implants (107–109) since the mechanical properties of porous biomaterials usually decline as the lattice structure's porosity rises (110).

3.4 Surface Porosity Condition and Corrosion

Generally, a potential relationship exists between a porous structure's relative density, elastic modulus and fatigue life. Higher porosity leads to a lower absolute stress value for the same number of cycles to failure (10). Recent works (111–113) have utilised porous metal to examine the impact of porous materials on biological behaviour. This work (114) has shown that bone ingrowth is impacted by porosity, pore size and interconnected pore throat size, utilising four porous titanium implants produced by the powder-sintering technique. The study also concluded that pores

© 2024 Johnson Matthey

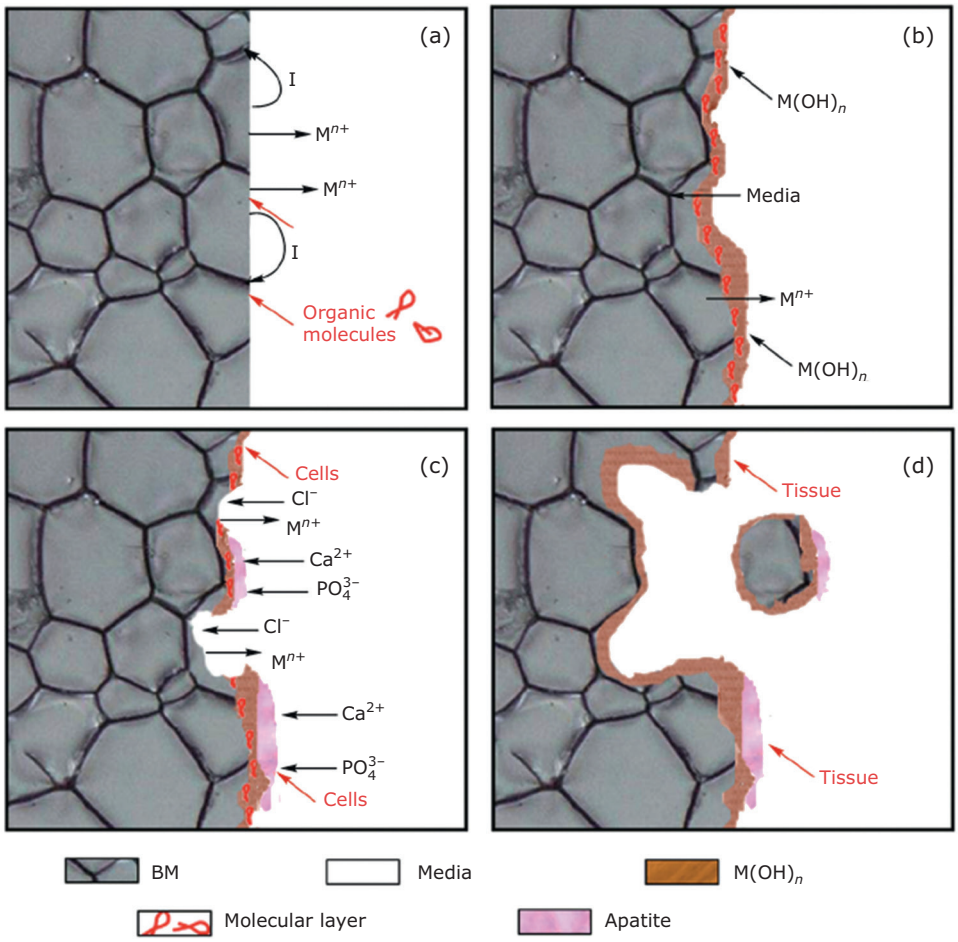

Fig. 6. Biocorrosion development within the medium interface of both implants and hosting physiological environments. Reprinted from (100), Copyright (2014), with permission from Elsevier

with narrow throats are undesirable for bone development. Porous titanium produced by powder-sintering processes, on the other hand, displayed variability in terms of pore size and pore throat size. In addition, weight and porosity may also be affected by the energy density of the source power (laser, electron beam). As the energy density increases, the weight and density increase. Following Barile *et al*., corrosion testing of 316L stainless steel produced by SLM revealed slightly varied corrosion tendencies depending on the energy density used. However, the limited distribution of flaws within the samples deposited at maximum energy meant they usually displayed minimal corrosion and good tensile characteristics (115). Dargusch *et al*. investigated the effect of LENS processing on the microstructure and biocorrosion performance of porous titanium alloy in comparison with conventional titanium alloy. The conventional implant possessed lower corrosion resistance than the AM one in Hank's solution, which can be explained by the microstructure and composition of alloys influenced by the fabrication method (83).

Optimising the parameters of the metal AM process remains an overriding challenge to improve the function of medical implants. This is more challenging for porous structures in terms of design, which requires careful determination of shape, composition, size and porosity (10). These characteristics simultaneously affect porous metallic biomaterials' mechanical properties and biological performance, including nutrient transport and bone growth (41). Nonetheless, their protection from tribocorrosion (consumption in relationship with mechanical erosion) and biocorrosion (corrosion in association with biological degradation and physiological environment) has received limited attention, which is the goal of this review.

4. Biocorrosion Constraints Within AM Porous Implants

The implant surface interacts with the surrounding environment of the human body which contains water, complex organic compounds and dissolved gasses and triggers chemical reactions to cause

© 2024 Johnson Matthey

implant degradation. Interaction with 316L stainless steel implants results in the release of Fe^{3+}, Cr^{2+} and Ni^{+} ions and the appearance of diseases like allergies and cancer (116, 117). These implant defects must be repaired and filled during revision operations with new structures to which new prosthesis parts are connected and protected (118). Preferably, these replacement materials should offer initial fixation along with long-term stability for the surrounding prosthesis. In addition, metallic biomaterials for implants with low carbon content can produce a passive layer to protect them from corrosive attacks (116). So far, the corrosion of dense metallic and biodegradable implants has been discussed. However, porous implants have recently been subjected to intense research.

There have been several papers reviewing the AM of bio-inert dense metals mainly from the materials processing and surface reactions viewpoint (23, 30, 119). The corrosion of porous implants fabricated by AM, such as titanium, stainless steel, chrome (cobalt-chromium) and tantalum, and their behaviour *via* corrosion, have recently shown up in the literature (120). AM materials can uphold a steady-state equilibrium between mechanical depassivation and electrochemical repassivation processes (higher passivation ability) (36). Schaller *et al*. (103) used PBF to fabricate 17-4 PH stainless steel porous structures. Microstructure evolution into SBF of 0.6 M sodium chloride solution was studied. Electrochemical reactions and measurements showed a reduced passivity range with active corrosion above larger pore sizes ≥50 µm compared to the characteristics of natural rough surface (103). Numerous studies have also demonstrated the inherent porous nature of stainless steel alloys to reduce passivity and increase corrosion susceptibility (121).

Table III summarises studies that explore this novel approach to increase the corrosion resistance of porous implants with AM techniques. Zhou examined the corrosion behaviour of titanium alloys produced additively by SLM with various microstructures (124). The results issued from potentiodynamic polarisation indicated that the Ti-13Nb-13Zr alloy has the highest corrosion potential compared with commercially pure titanium (CP-Ti) and Ti-6Al-4V. This could be explained by the presence of niobium pentoxide which is more chemically stable than vanadium pentoxide. Vanadium or niobium and solid layers of niobium oxide and zirconia exist in the passive titanium dioxide layers during corrosion, which could reduce Cl^{-} ingress into the oxide layer and increase the structural integrity of the oxide film (124). Other works studied the wear resistance of SLM-manufactured CP–Ti and EBM-manufactured Ti4V6 gyroid scaffolds (125). It was found that the corrosion behaviour of the AM parts was the most challenging issue to be resolved.

The determination of parameters, characterisation techniques and surface modification enable corrosion to be detect and overcome. The inorganic ions in physiological solutions usually influence degradation due to specific temperature conditions in *in vitro* studies (100). The sintering temperature and time could significantly change the coating/substrate interface reactions and thus influence coating adhesion. In contrast, high temperatures could create porosity in the inner part of a coating where the coating directly binds to the substrate, therefore resulting in a lower degree of densification which causes a reduction in the strength of the coating-substrate bonding (126) and overcomes undesirable surface defects and exposure of the M(OH) layer in physiological environments (**Figure 7**).

Magnesium, iron and zinc and their alloys are the only AM biodegradable porous metallic materials tested against corrosion (**Table III**). Bio-inert and biodegradable porous metals, including magnesium and zinc, have low melting and boiling temperatures and high chemical activity. This generates an essential set of problems in PBF. Defects such as voids, lack of fusion, rough surface, significant residual stresses and distortions that may arise under poor processing conditions (23) make the surface vulnerable to biocorrosion. Up to now, there has been a dearth of study into the corrosion attack of porous metals in biomedical applications. As a result, more studies are required better to understand the corrosion mechanism of AM porous metallic implants.

5. Future Trends and Perspectives

In the coming years, AM of porous implants will increase rapidly over other techniques (128, 129) due to their ability to address reconstructive challenges beyond standard implant scope. However, some significant limits remain in the design and optimisation of AM process parameters and degradation after *in vivo* implantation. Various unit cell structures have been presented in the literature and the methodology of structural design

 © 2024 Johnson Matthey

Table III Corrosion Behaviour of Some Additively Manufactured Metallic Porous Implants

Process	Material, unit cell	Porosity, %	Pore size, µm	Exposition period, days	Weight loss, %	Testing medium	Intensity corrosion rate, CRI, mm year^{-1}	Corrosion rate potential, CRE, mA cm^{-2}	References
SLM	Magnesium, diamond	67	600	28	20.70	r-SBF	0.23	21–61	(25)
SLM	Iron, diamond	80	800	28	3.1	r-SBF	0.03	102.8±19	(122)
SLM	Zinc, diamond	72.6	700	28	11.9	r-SBF	0.17	–	(123)
PBF	Zinc, diamond	62	600	28	3.8	Air & r-SBF	0.07	45±2	(21)
PBF	UNS S17400 (17-4 precipitation-hardenable), dense	–	–	1	–	0.6 M NaCl	–	2.73 × 10^{-6} ±4 × 10^{-11}	(103)

and the mechanical properties of several implants have also been systematically evaluated. Future work should be directed toward understanding the biological behaviour and degradation of the porous implant as affected by unit cell types, geometrical parameters and the passivation layer. Cazzola *et al*. proposed a combination of biochemical and physical approaches to optimise the biofunctions of AM implants and maximise bone regeneration (130). The importance of the degradation behaviour of metallic implants has been realised in recent years. However, the study of corrosion within porous structures has not yet been developed. With the maturation of metal AM technology, research trends will focus on corrosion mechanisms and orthopaedic implant failures inside the human body. In addition, understanding the mechanisms of biocorrosion at the material-tissue interface and investigating the modified surface will provide robust means for researchers to select proper biomaterials and surface modification techniques.

6. Conclusion

In the current review, we have explored exciting and novel areas of discovery related to porous metallic implants, their manufacture and their potential to resist corrosion. In addition to demonstrating the wide possibilities in this field, we have outlined their limitations and shortcomings. Metal AM technology produces implants that mimic the anatomy of the patient. It also allows the manufacture of porous scaffolds. However, the lack of long-term clinical results remains the main concern for the development of AM in orthopaedic implants. Surface modifications are often performed on biomedical implants to improve corrosion resistance, wear resistance, surface texture and biocompatibility. The literature illustrates limited data with respect to understanding the interfacial phenomena generated between the porous implant and the host bone by describing various behaviours occurring *in vivo*. It implies chemical interaction between substances and oxide-coated metal surfaces (passive film) and the need to combine surface analysis with implant regeneration to achieve optimum results. Numerous advances have been made in biomaterials and tissue engineering; however, the complexity of human tissues and organs means that further studies will be required to unscramble the mechanisms and interactions between tissues, cells and porous metallic implants after implantation.

© 2024 Johnson Matthey

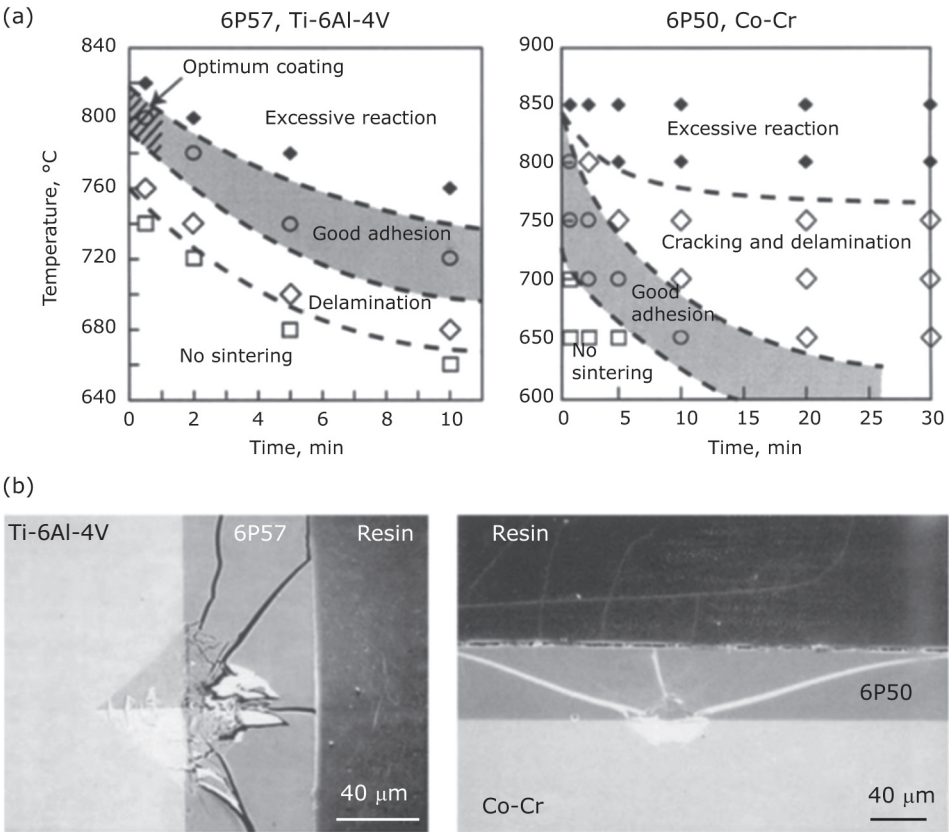

Fig. 7. (a) Effects of sintering time and temperature on the coating adhesion of bioactive glass 6P57 on Ti-6Al-14V and 6P50 on cobalt-chromium; (b) the corresponding Vickers indentations at the glass interfaces performed in ambient air that shows good glass-metal adhesion without delamination of coating. Reprinted from (127), Copyright (2003), with permission from Elsevier

Conflicts of Interest

There are no conflicts to declare. The authors alone are responsible for the content and writing of this review.

Author Contributions

Salwa El Baakili: conceptualisation, investigation, writing original draft; Patrick Munyensanga: conceptualisation, investigation, writing initial draft; Meriame Bricha: conceptualisation, writing, reviewing and editing; Khalil El Mabrouk: validation, writing, reviewing and editing.

Acknowledgments

This research was supported by Euromed University of Fez, Morocco.

References

1. A. Balamurugan, S. Rajeswari, G. Balossier, A. H. S. Rebelo, J. M. F. Ferreira, *Mater. Corros.*, 2008, **59**, (11), 855
2. K. K. L. Bhishagratna, "An English Translation of The Sushruta Samhita: Based on the Original Sanskrit Text", K. K. L. Bhishagratna, Calcutta, India, 1907
3. S. F. Hulbert, L. L. Hench, D. Forbers, L. S. Bowman, *Ceram. Int.*, 1982, **8**, (4), 131
4. E. Radin, *J. Bone Joint Surg.*, 1989, **71**, (6), 957
5. P. Munyensanga, P. Paryanto, M. N. A. Aziz, *ROTASI*, 2019, **20**, (4), 249
6. W. S. W. Harun, M. S. I. N. Kamariah, N. Muhamad, S. A. C. Ghani, F. Ahmad, Z. Mohamed, *Powder Technol.*, 2018, **327**, 128
7. L.-C. Zhang, L.-Y. Chen, *Adv. Eng. Mater.*, 2019, **21**, (4), 1801215
8. L. Thijs, F. Verhaeghe, T. Craeghs, J. Van Humbeeck, J.-P. Kruth, *Acta Mater.*, 2010, **58**, (9), 3303
9. 'Additive Manufacturing: General Principles: Fundamentals and Vocabulary', ISO/ASTM 52900:2021, International Organization for Standardization, Geneva, Switzerland, November, 2021
10. A. A. Zadpoor, *J. Mater. Chem. B*, 2019, **7**, (26), 4088
11. A. Zadpoor, *Int. J. Mol. Sci.*, 2017, **18**, (8), 1607
12. J.-H. Chen, C. Liu, L. You, C. A. Simmons, *J. Biomech.*, 2010, **43**, (1), 108
13. X. Li, X.-Y. Ma, Y.-F. Feng, L. Wang, C. Wang,

 © 2024 Johnson Matthey

Compos. Sci. Technol., 2015, **117**, 78

14. C. Zhang, L. Zhang, L. Liu, L. Lv, L. Gao, N. Liu, X. Wang, J. Ye, *J. Orthop. Surg. Res.*, 2020, **15**, 40
15. J. A. Semba, A. A. Mieloch, J. D. Rybka, *Bioprinting*, 2020, **18**, e00070
16. 'Standard Specification for Wrought Cobalt-28Chromium-6Molybdenum Alloys for Surgical Implants (UNS R31537, UNS R31538, and UNS R31539)', ASTM F1537-20, ASTM International, West Conshohocken, USA, 29th April, 2020
17. M. Kaur, K. Singh, *Mater. Sci. Eng.: C*, 2019, **102**, 844
18. 'How to Design Parts for Metal 3D Printing', HUBS, Amsterdam, The Netherlands: https://www.hubs.com/knowledge-base/how-design-parts-metal-3d-printing/ (Accessed on 24th Otober 2023)
19. S. Attarilar, M. Ebrahimi, F. Djavanroodi, Y. Fu, L. Wang, J. Yang, *Int. J. Bioprint.*, 2021, **7**, (1), 306
20. N. Dai, L.-C. Zhang, J. Zhang, Q. Chen, M. Wu, *Corros. Sci.*, 2016, **102**, 484
21. Y. Li, W. Li, F. S. L. Bobbert, K. Lietaert, J. Dong, M. A. Leeflang, J. Zhou, A. A. Zadpoor, *Acta Biomater.,* 2020, **106**, 439
22. Y. Cao, P. Bai, F. Liu, X. Hou, Y. Guo, *Materials*, 2020, **13**, (2), 340
23. Y. Li, H. Jahr, J. Zhou, A. Abbas, *Acta Biomater.*, 2020, **115**, 29
24. T. DebRoy, H. L. Wei, J. S. Zuback, T. Mukherjee, J. W. Elmer, J. O. Milewski, A. M. Beese, A. Wilson-Heid, A. De, W. Zhang, *Prog. Mater. Sci.*, 2018, **92**, 112
25. Y. Li, J. Zhou, P. Pavanram, M. A. Leeflang, L. I. Fockaert, B. Pouran, N. Tümer, K.-U. Schröder, J. M. C. Mol, H. Weinans, H. Jahr, A. A. Zadpoor, *Acta Biomater.*, 2018, **67**, 378
26. W. E. Frazier, *J. Mater. Eng. Perform.*, 2014, **23**, (6), 1917
27. M. Munsch, 'Laser Additive Manufacturing of Customized Prosthetics and Implants for Biomedical Applications', in "Laser Additive Manufacturing: Materials, Design, Technologies, and Applications", ed. M. Brandt, ch. 15, Woodhead Publishing Series in Electronic and Optcal Materials No. 88, Elsevier Ltd, Duxford, UK, 2017, pp. 399–420
28. F. Suska, G. Kjeller, P. Tarnow, E. Hryha, L. Nyborg, A. Snis, A. Palmquist, *J. Oral Maxillofac. Surg.*, 2016, 74, (8), 1706.e1
29. B. AlMangour, D. Grzesiak, J.-M. Yang, *Powder Technol.*, 2017, **309**, 37
30. Y. Qin, P. Wen, H. Guo, D. Xia, Y. Zheng, L. Jauer, R. Poprawe, M. Voshage, J. H. Schleifenbaum, *Acta Biomater.*, 2019, **98**, 3
31. X.-Y. Zhang, G. Fang, J. Zhou, *Materials*, 2017, **10**, (1), 50
32. B. Utela, D. Storti, R. Anderson, M. Ganter, *J. Manuf. Process.*, 2008, **10**, (2), 96
33. C. Y. Yap, C. K. Chua, Z. L. Dong, Z. H. Liu, D. Q. Zhang, L. E. Loh, S. L. Sing, *Appl. Phys. Rev.*, 2015, **2**, (4), 041101
34. A. Bandyopadhyay, K. D. Traxel, M. Lang, M. Juhasz, N. Eliaz, S. Bose, *Mater. Today*, 2022, **52**, (January–February), 207
35. W. Ge, C. Guo, F. Lin, *Proc. Eng.*, 2014, **81**, 1192
36. Y. Qin, P. Wen, D. Xia, H. Guo, M. Voshage, L. Jauer, Y. Zheng, J. H. Schleifenbaum, Y. Tian, *Addit. Manuf.*, 2020, **33**, 101134
37. C. N. Kuo, C. K. Chua, P. C. Peng, Y. W. Chen, S. L. Sing, S. Huang, Y. L. Su, *Virtual Phys. Prototyp.*, 2020, **15**, (1), 120
38. N. Koju, S. Niraula, B. Fotovvati, *Metals*, 2022, **12**, (4), 687
39. X. Xin, J. Chen, N. Xiang, Y. Gong, B. Wei, *Dent. Mater.*, 2014, **30**, (3), 263
40. S. Limmahakhun, A. Oloyede, K. Sitthiseripratip, Y. Xiao, C. Yan, *Mater. Des.*, 2017, **114**, 633
41. Z. Linxi, Y. Quanzhan, Z. Guirong, Z. Fangxin, S. Gang, Y. Bo, *China Found.,* 2014, **11**, (4), 322
42. M. Folkman, A. Becker, I. Meinster, M. Masri, Z. Ormianer, *Sci. Rep.*, 2020, **10**, 12446
43. H. Wang, K. Su, L. Su, P. Liang, P. Ji, C. Wang, *J. Mech. Behav. Biomed. Mater.*, 2018, **88**, 488
44. G. Chen, C. Dong, L. Yang, Y. Lv, *ACS Appl. Mater. Interfaces*, 2015, **7**, (29), 15790
45. M. Dadkhah, M. H. Mosallanejad, L. Iuliano, A. Saboori, *Acta Metall. Sin. (English Lett.)*, 2021, **34**, (9), 1173
46. S. Singh, S. Ramakrishna, R. Singh, *J. Manuf. Process.*, 2017, **25**, 185
47. G. Del Guercio, M. Galati, A. Saboori, *Met. Mater. Int.*, 2021, **27**, (1), 55
48. L.-C. Zhang, Y. Liu, S. Li, Y. Hao, *Adv. Eng. Mater.*, 2018, **20**, (5), 1
49. A. M. Crovace, L. Lacitignola, D. M. Forleo, F. Staffueru, E. Francioso, A. Di Meo, J. Becerra, A. Crovace, L. Santos-Ruiz, *Animals*, 2020, **10**, (8), 1389
50. P. Szymczyk-Ziółkowska, G. Ziółkowski, V. Hoppe, M. Rusińska, K. Kobiela, M. Madeja, R. Dziedzic, A. Junka, J. Detyna, *J. Manuf. Process.*, 2022, **76**, 175
51. T. D. Ngo, A. Kashani, G. Imbalzano, K. T. Q. Nguyen, D. Hui, *Compos. Part B: Eng.*, 2018, **143**, 172

 © 2024 Johnson Matthey

52. N. Ohtsu, S. Suginishi, M. Hirano, *Appl. Surf. Sci.*, 2017, **405**, 215
53. D. Kong, C. Dong, X. Ni, X. Li, *npj Mater. Degrad.*, 2019, **3**, 24
54. O. Cissé, O. Savadogo, M. Wu, L'H. Yahia, *J. Biomed. Mater. Res.*, 2002, **61**, (3), 339
55. X. Zhao, S. Li, M. Zhang, Y. Liu, T. B. Sercombe, S. Wang, Y. Hao, R. Yang, L. E. Murr, *Mater. Des.*, 2016, **95**, 21
56. Y. Yang, Y. J. Liu B, J. Chen, H. L. Wang, Z. Q. Zhang, Y. J. Lu, S. Q. Wu, J. X. Lin, *Mater. Sci. Eng: A*, 2017, **707**, 548
57. J.-R. Chen, W.-T. Tsai, *Electrochim. Acta*, 2011, **56**, (4), 1746
58. J. Stendal, O. Fergani, H. Yamaguchi, N. Espallargas, *J. Bio- Tribo-Corros.*, 2018, **4**, (1), 9
59. P. Mutombo, N. Hackerman, *J. Solid State Electrochem.*, 1997, **1**, (3), 194
60. D. Gilroy, B. E. Conway, *J. Phys. Chem.*, 1965, **69**, (4), 1259
61. A. Dehghanghadikolaei, H. Ibrahim, A. Amerinatanzi, M. Hashemi, N. S. Moghaddam, M. Elahinia, *J. Mater. Sci.*, 2019, **54**, (9), 7333
62. A. Dehghanghadikolaei, B. Fotovvati, *Materials*, 2019, **12**, (11), 1795
63. I. Azzouz, J. Faure, K. Khlifi, A. C. Larbi, H. Benhayoune, *Coatings*, 2020, **10**, (12), 1192
64. M. Saini, *World J. Clin. Cases*, 2015, **3**, (1), 52
65. A. Seyeux, S. Zanna, P. Marcus, 'Surface Analysis Techniques for Investigating Biocorrosion', in "Understanding Bicorrosion: Fundamentals and Applications", eds. T. Liengen, D. Féron, R. Basséguy and I. B. Beech, ch. 8, European Federation of Corrosion Publications No. 66, Woodhead Publishing Ltd, Sawston, UK, 2014, pp. 197–212
66. D. Hong, D.-T. Chou, O. I. Velikokhatnyi, A. Roy, B. Lee, I. Swink, I. Issaev, H. A. Kuhn, P. N. Kumta, *Acta Biomater.*, 2016, **45**, 375
67. M. Bryant, A. Neville, *Orthop. Trauma*, 2016, **30**, (3), 176
68. S. Ali, A. M. A. Rani, Z. Baig, S. W. Ahmed, G. Hussain, K. Subramaniam, S. Hastuty, T. V. V. L. N. Rao, *Corros. Rev.*, 2020, **38**, (5), 381
69. K. Prasad, O. Bazaka, M. Chua, M. Rochford, L. Fedrick, J. Spoor, R. Symes, M. Tieppo, C. Collins, A. Cao, D. Markwell, K. Ostrikov, K. Bazaka, *Materials*, 2017, **10**, (8), 884
70. N. J. Hallab, J. J. Jacobs, 'Orthopedic Applications', in "Biomaterials Science: An Introduction to Materials in Medicine", eds. B. D. Ratner, A. S. Hoffman, F. J. Schoen, J. E. Lemons, ch. II.5.6, Elsevier Inc, Waltham, USA, 2013, pp. 841–882
71. 'Pitting Corrosion', Association for Materials Protection and Peformance (AMPP), Houston, USA: https://www.ampp.org/technical-research/impact/corrosion-basics/group-1/pitting-corrosion (Accessed on 20th October 2023)
72. 'Eight Forms of Corrosion', Corrosion Doctor: https://corrosion-doctors.org/Corrosion-History/Eight.htm (Accessed on 20th October 2023)
73. K. J. Vetter, *Electrochim. Acta*, 1971, **16**, (11), 1923
74. S. V. Dorozhkin, *Acta Biomater.*, 2014, **10**, (7), 2919
75. E. Radin, *J. Bone Joint Surg*., 1989, **71**, (6), 957
76. S. Bano, M. Akhtar, M. Yasir, M. S. Maqbool, A. Niaz, A. Wadood, M. A. Ur. Rehman, *Gels*, 2021, **7**, (2), 34
77. A. Cinitha, P. K. Umesha, N. R. Iyer, *KSCE J. Civ. Eng.*, 2014, **18**, (6), 1735
78. B. Singh, G. Singh, B. S. Sidhu, *J. Therm. Spray Technol.*, 2018, **27**, (8), 1401
79. J. H. U. Brown, J. E. Jacobs, L. Stark, "Biomedical Engineering", F. A. Davis Co, Philadelphia, USA, 1970
80. L.-C. Zhang, H. Attar, *Adv. Eng. Mater.*, 2016, **18**, (4), 463
81. A. Ataee, Y. Li, C. Wen, *Acta Biomater.*, 2019, **97**, 587
82. F. Bartolomeu, M. Buciumeanu, E. Pinto, N. Alves, F. S. Silva, O. Carvalho, G. Miranda, *Trans. Nonferrous Met. Soc. China*, 2017, **27**, (4), 829
83. M. S. Dargusch, G. Wang, D. Kent, M. Bermingham, J. Venezuela, J. E. Frith, Z. Yu, S. Yu, Z. Shi, *ACS Biomater. Sci. Eng*., 2019, **5**, (11), 5844
84. B. Zhao, H. Wang, N. Qiao, C. Wang, M. Hu, *Mater. Sci. Eng.: C*, 2017, **70**, (1), 832
85. M. K. Zadeh, M. Yeganeh, M. T. Shoushtari, H. Ramezanalizadeh, F. Seidi, *Mater. Today Commun.*, 2022, **31**, 103502
86. E. Liverani, S. Toschi, L. Ceschini, A. Fortunato, *J. Mater. Process. Technol.*, 2017, **249**, 255
87. R. A. Gittens, R. Olivares-Navarrete, R. Tannenbaum, B. D. Boyan, Z. Schwartz, *J. Dent. Res*., 2011, **90**, (12), 1389
88. R. B. Heimann, *Metals*, 2017, **7**, (11), 468
89. H. H. Hernández, A. M. R. Reynoso, J. C. T. González, C. O. G. Morán, J. G. M. Hernández, A. M. Ruiz, J. M. Hernández, R. O. Cruz, 'Electrochemical Impedance Spectroscopy (EIS): A Review Study of Basic Aspects of the Corrosion Mechanism

 © 2024 Johnson Matthey

Applied to Steels', in "Electrochemical Impedance Spectroscopy", eds. M. El-Azazy, M. Min, P. Annus, IntechOpen, London, UK, 2020, 35 pp

90. J. Brezinová, R. Hudák, A. Guzanová, D. Draganovská, G. Ižaríková, J. Koncz, *Metals*, 2016, **6**, (7), 171
91. J. J. Marattukalam, A. K. Singh, S. Datta, M. Das, V. K. Balla, S. Bontha, S. K. Kalpathy, *Mater. Sci. Eng.: C*, 2015, **57**, 309
92. 'Sand Inclusion, Sand Hole', Liaoning Borui Machinery Co Ltd, Dandong, China, 26th September, 2021
93. M. H. Shaeri Karimi, M. Yeganeh, S. R. Alavi Zaree, M. Eskandari, *Opt. Laser Technol.*, 2021, **138**, 106918
94. T. Inoue, 'Metallo-Thermo-Mechanics–Application to Quenching', in "Handbook of Residual Stress and Deformation of Steel", eds. G. Totten, M. Howes, T. Inoue, ASM International, Materials Park, USA, 2002, pp. 296–311
95. A. Boschetto, L. Bottini, F. Veniali, *J. Mater. Process. Technol.*, 2017, **241**, 154
96. G. Strano, L. Hao, R. M. Everson, K. E. Evans, *J. Mater. Process. Technol.*, 2013, **213**, (4), 589
97. E. Gerashi, R. Alizadeh, T. G. Langdon, *J. Magnes. Alloy.*, 2022, **10**, (2), 313
98. J. Wang, H. Li, *Mater. Res. Express*, 2019, **6**, (6), 066508
99. A. Leon, E. Aghion, *Mater. Charact.*, 2017, **131**, 188
100. Y. F. Zheng, X. N. Gu, F. Witte, *Mater. Sci. Eng. R: Rep.*, 2014, **77**, 1
101. A. L. Maximenko, E. A. Olevsky, *Scr. Mater.*, 2018, **149**, 75
102. G. Sander, S. Thomas, V. Cruz, M. Jurg, N. Birbilis, X. Gao, M. Brameld, C. R. Hutchinson, *J. Electrochem C. Soc*, 2017, **164**, (6), C250
103. R. F. Schaller, J. M. Taylor, J. Rodelas, E. J. Schindelholz, *Corrosion*, 2017, **73**, (7), 796
104. H. Liang, Y. Yang, D. Xie, L. Li, N. Mao, C. Wang, Z. Tian, Q. Jiang, L. Shen, *J. Mater. Sci. Technol.*, 2019, **35**, (7), 1284
105. Q. Ran, W. Yang, Y. Hu, X. Shen, Y. Yu, Y. Xiang, K. Cai, *J. Mech. Behav. Biomed. Mater.*, 2018, **84**, 1
106. R. Wauthle, J. van der Stok, S. Amin Yavari, J. Van Humbeeck, J.-P. Kruth, A. A. Zadpoor, H. Weinans, M. Mulier, J. Schrooten, *Acta Biomater.*, 2015, **14**, 217
107. A. H. Maamoun, Y. F. Xue, M. A. Elbestawi, S. C. Veldhuis, *Materials*, 2018, **11**, (12), 2343
108. V. Cruz, Q. Chao, N. Birbilis, D. Fabijanic, P. D. Hodgson, S. Thomas, *Corros. Sci.*, 2020, **164**, 108314
109. S. Gorsse, C. Hutchinson, M. Gouné, R. Banerjee, *Sci. Technol. Adv. Mater.*, 2017, **18**, (1), 584
110. M. F. Ashby, *Philos. Trans. R. Soc. A*, 2006, **364**, (1838), 15
111. N. Taniguchi, S. Fujibayashi, M. Takemoto, K. Sasaki, B. Otsuki, T. Nakamura, T. Matsushita, T. Kokubo, S. Matsuda, *Mater. Sci. Eng.: C*, 2016, **59**, 690
112. B. Otsuki, M. Takemoto, S. Fujibayashi, M. Neo, T. Kokubo, T. Nakamura, *Biomaterials*, 2006, **27**, (35), 5892
113. S. Van Bael, Y. C. Chai, S. Truscello, M. Moesen, G. Kerckhofs, H. Van Oosterwyck, J.-P. Kruth, J. Schrooten, *Acta Biomater.*, 2012, **8**, (7), 2824
114. S. Haeri, Y. Wang, O. Ghita, J. Sun, *Powder Technol.*, 2017, **306**, 45
115. C. Barile, C. Casavola, S. L. Campanelli, G. Renna, *Eng. Fail. Anal.*, 2019, **95**, 273
116. D. C. Hansen, *Electrochem. Soc. Interface*, 2008, **17**, (2), 31
117. T. Kraus, S. F. Fischerauer, A. C. Hänzi, P. J. Uggowitzer, J. F. Löffler, A. M. Weinberg, *Acta Biomater.*, 2012, **8**, (3), 1230
118. K. Moghadasi, M. S. Mohd Isa, M. A. Ariffin, M. Z. Mohd jamil, S. Raja, B. Wu, M. Yamani, M. R. Bin Muhamad, F. Yusof, M. F. Jamaludin, M. S. bin Ab Karim, B. binti Abdul Razak, N. bin Yusoff, *J. Mater. Res. Technol.*, 2022, **17**, 1054
119. I. D. Learmonth, C. Young, C. Rorabeck, *Lancet*, 2007, **370**, (9597), 1508
120. S. M. Ahmadi, R. Hedayati, Y. Li, K. Lietaert, N. Tümer, A. Fatemi, C. D. Rans, B. Pouran, H. Weinans, A. A. Zadpoor, *Acta Biomater.*, 2018, **65**, 292
121. E. Otero, A. Pardo, E. Sáenz, M. V. Utrilla, F. J. Pérez, *Can. Metall. Quart.*, 1997, **36**, (1), 65
122. Y. Li, H. Jahr, K. Lietaert, P. Pavanram, A. Yilmaz, L. I. Fockaert, M. A. Leeflang, B. Pouran, Y. Gonzalez-Garcia, H. Weinans, J. M. C. Mol, J. Zhou, A. A. Zadpoor, *Acta Biomater.*, 2018, **77**, 380
123. Y. Li, P. Pavanram, J. Zhou, K. Lietaert, F. S. L. Bobbert, Y. Kubo, M. A. Leeflang, H. Jahr, A. A. Zadpoor, *Biomater. Sci.*, 2020, **8**, (9), 2404
124. L. Zhou, T. Yuan, J. Tang, J. He, R. Li, *Opt. Laser Technol.*, 2019, **119**, 105625
125. A. Ataee, Y. Li, M. Brandt, C. Wen, *Acta Mater.*, 2018, **158**, 354
126. J. N. Oliver, Y. Su, X. Lu, P.-H. Kuo, J. Du, D. Zhu, *Bioact. Mater.*, 2019, **4**, 261
127. S. Lopez-Esteban, E. Saiz, S. Fujino, T. Oku, K. Suganuma, A. P. Tomsia, *J. Eur. Ceram. Soc.*,

 © 2024 Johnson Matthey

2003, **23**, (15), 2921

128. J. Harrop, '3D Printing Materials 2015–2025: Status, Opportunities, Market Forecasts: Pricing, Properties and Projections for Materials Including Photopolymers, Thermoplastics and Metal Powders', IDTechEx, Cambridge, UK: https://www.idtechex.com/en/research-report/3d-printing-materials-2015-2025-status-opportunities-market-forecasts/416 (Accessed on 20th October 2023)
129. P. Kocovic, 'History of Additive Manufacturing', in "3D Printing and Its Impact on the Production of Fully Functional Components: Emerging Research and Opportunities", ch. 1, IGI Global, Hershey, USA, 2017, pp. 1–24
130. M. Cazzola, S. Ferraris, F. Boschetto, A. Rondinella, E. Marin, W. Zhu, G. Pezzotti, E. Vernè, S. Spriano, *Int. J. Mol. Sci.*, 2018, **19**, (8), 2255

The Authors

Salwa El Baakili is a PhD student at the Euromed University of Fez. She graduated from the National School of Applied Sciences (ENSA), Morocco, with a degree in Chemical Engineering in 2019. Her research topics include biomaterials for bone regeneration and tissue engineering. She is interested in electrophoretic deposition (EPD), the electrochemical behaviour of metallic implants, electrospinning (ES) and the synthesis of inorganic biomaterials.

Patrick Munyensanga is a PhD student at the Euromed University of Fez, specialising in biomaterials and additive manufacturing. His research primarily centres on porous implants for bone regeneration. He is also profoundly interested in smart manufacturing, additive manufacturing and advanced nanocoating applications to improve biocorrosion resistance in additively manufactured porous metallic structures. He holds a Master of Engineering from Diponegoro University, Indonesia, and a Bachelor of Science in Engineering from the University of Rwanda, focusing on mechanical and materials engineering.

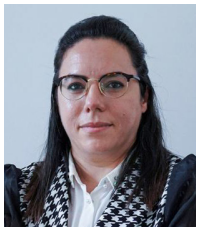

Meriame Bricha obtained her Doctorate in Physico-Chemical Materials, Ceramics and Nanocomposites at the Faculty of Sciences of Agdal in Rabat, Morocco, in 2013, in collaboration with Ceramic Biomaterials Center at iNANOTECH (MAScIR), Rabat. She is Associate Professor at The Euromed Polytechnic School, Euromed University of Fez. Her research interests are ceramics, bioglass and the biocorrosion of parts from metal additive manufacturing by SLM after surface treatment by electrophoretic deposition for bone tissue regeneration.

Khalil El Mabrouk obtained his PhD in Chemical Engineering in 2005 at Laval University, Canada; postdoctoral research at Queen's University, Canada and Dow Chemical New Jersey, USA. He was Research Director in the Moroccan Foundation for Advanced Science Innovation and Research from 2008 to 2013. Since 2013 he is Full Professor at The Euromed Polytechnic School, Euromed University of Fez, Morocco. His research interests are additive manufacturing, soft and hard tissue engineering, bone regeneration, wound healing and advanced materials for medical and aerospace applications.

 © 2024 Johnson Matthey